JGR Space Physics

RESEARCH ARTICLE
10.1029/2024JA033007

**Key Points:**
- A 3D global hybrid simulation at a realistic scale has been used to investigate the dayside ULF waves under a radial interplanetary magnetic field
- Pc 3 waves are self-consistently generated at the foreshock region and transmitted into the magnetosheath and magnetosphere
- Fluctuations in the magnetosheath exhibit a broad spectrum, and only lower frequency compressional waves are effectively transmitted into the magnetosphere

**Supporting Information:**
Supporting Information may be found in the online version of this article.

**Correspondence to:**
J. Sun and Q. Lu,
sunjicheng@pric.org.cn;
qmlu@ustc.edu.cn

**Citation:**
Sun, J., Ren, J., Lu, Q., Zhang, B., & Yang, H. (2024). The transmission of Pc 3 waves from the foreshock into the Earth's magnetosphere: 3D global hybrid simulation. *Journal of Geophysical Research: Space Physics*, *129*, e2024JA033007. https://doi.org/10.1029/2024JA033007

Received 28 JUN 2024
Accepted 17 OCT 2024



# The Transmission of Pc 3 Waves From the Foreshock Into the Earth's Magnetosphere: 3D Global Hybrid Simulation

**Jicheng Sun[1], Junyi Ren[2], Quanming Lu[2], Beichen Zhang[1], and Huigen Yang[1]**

[1]MNR Key Laboratory for Polar Science, Polar Research Institute of China, Shanghai, China, [2]CAS Key Laboratory of Geospace Environment, Department of Geophysics and Planetary Science, University of Science and Technology of China, Hefei, China

**Abstract** Although initially it was presumed that foreshock waves would propagate directly into the dayside magnetosphere, observational evidence for sinusoidal Pc3 waves in the downstream of quasi-parallel shocks is scarce. The transmission of these waves from the foreshock into the magnetosphere remains uncertain. In this paper, we employ a 3D global hybrid simulation at a realistic scale to explore the generation and transmission of the dayside ULF waves under a radial interplanetary magnetic field. Our findings demonstrate that the Pc3 waves are self-consistently generated in the foreshock region and then transmitted into the magnetosheath and magnetosphere. In the foreshock, the waves are excited at approximately 25 mHz and exhibit right-handed helicity in the plasma frame, characterizing them as quasi-parallel fast magnetosonic waves. In the magnetosphere, the fluctuating magnetic field is mainly parallel to the background magnetic field, which indicates the dominant wave modes are compressional. Fluctuations in the magnetosheath show a broader spectrum (10–100 mHz) compared to those in the magnetosphere and foreshock, potentially explaining the little observation of sinusoidal Pc3 waves in the magnetosheath. Additionally, only lower frequency compressional waves (below 30 mHz) are effectively transmitted into the dayside magnetosphere. Our simulation provides critical insights into the interactions between the solar wind and Earth's magnetosphere.

**Plain Language Summary** Ultralow frequency waves in the Pc3 range, with periods of 10–45 s, are frequently detected in the Earth's magnetosphere. These waves are thought to originate from ion foreshock regions upstream of Earth's quasi-parallel bow shock. They arise from ion beam instabilities triggered by the interaction between shock-reflected suprathermal ions and the incoming solar wind. While it was assumed that these Pc3 waves would directly enter the dayside magnetosphere, in-situ observations of sinusoidal Pc3 waves in the magnetosheath remain rare. This scarcity of evidence has left the mechanisms of their propagation into the magnetosphere unclear. This paper employs a 3D global hybrid simulation at a realistic scale to investigate how the Pc3 waves are transmited through the bow shock, magnetosheath, and into the magnetosphere under a radial interplanetary magnetic field. Our results indicate that the Pc3 waves are self-consistently generated in the foreshock and transmitted into the magnetosheath and magnetosphere, with only lower frequency compressional waves effectively propagating into the magnetosphere. Fluctuations in the magnetosheath exhibit a broader spectrum compared to those in the magnetosphere and foreshock.

## 1. Introduction

Ultralow frequency (ULF) waves in the Pc3 range, with periods between 10 and 45s, are widely observed in the foreshock (Le & Russell, 1996), magnetosphere (Engebretson et al., 1987; Takahashi et al., 1984), ionosphere (Heilig et al., 2007), and on the ground (Yeoman et al., 2012; Yumoto et al., 1985). These waves are believed to originate from the ion foreshock, which extends upstream of the Earth's quasi-parallel bow shock. In this region, the Pc3 waves are generated by ion beam instabilities resulting from the interaction between shock-reflected suprathermal ions and the incoming solar wind (Eastwood, Lucek, et al., 2005; Wilson, 2016). Due to their typical period, they are also referred to as "30-s waves" in the Earth's foreshock. These Pc3 waves, extending several Earth radii along their wave vector and featuring a wavelength of about one Earth radius, typically propagate at angles of 20–40° relative to the local magnetic field (Archer et al., 2005; Hoppe & Russell, 1983; Palmroth et al., 2015). They propagate sunwards at speeds near the local Alfven speed within the plasma frame, yet the faster solar wind flow convects them earthward into the shock. This convection process results in the reversal of their polarization, changing from right-handed in the plasma frame to left-handed in the spacecraft frame. Exhibiting large amplitudes comparable to the background magnetic field, the Pc3 waves significantly affect the dynamics of Earth's bow shock by modulating the shape of the shock front (Burgess, 1995; Greenstadt & Mellott, 1985), impacting particle reflection at the shock (Wu et al., 2015), and inducing oblique bow shock reformation (Liu et al., 2021). Moreover, recent spacecraft-imager conjunction studies by Motoba et al. (2019) have demonstrated that these Pc3 waves are a primary factor controlling the frequency of daytime auroral pulsations.

Numerous studies have demonstrated that the occurrence and frequency of Pc3 waves depend strongly on solar wind conditions such as velocity and density, as well as the interplanetary magnetic field (IMF) orientation (Bier et al., 2014; Regi et al., 2014; Yumoto et al., 1984). Specifically, the emergence of magnetospheric Pc3 waves is intricately linked to the foreshock's position, which is governed by the direction of the IMF, particularly its cone angle $\theta_{Bx}$, between the IMF and the Sun-Earth line. Smaller cone angles, allowing the foreshock to extend upstream of the subsolar magnetosphere, foster more intense Pc3 wave activity (Chi et al., 1994; Heilig et al., 2007; Yumoto et al., 1985). Heilig et al. (2007) specifically noted a marked decline in the logarithmic wave power spectral density for cone angles exceeding approximately 35° in a statistical analysis based on dayside compressional Pc3 pulsations observed by the low-altitude CHAMP spacecraft. Regarding the frequency of these waves, Takahashi et al. (1984) developed a theoretical formula for foreshock wave frequency as $f(mHz) = 7.6B_{IMF}(nT)cos^2\theta_{Bx}$. Direct measurements from ISEE 1 and 2 upstream of the bow shock, undertaken by Russell and Hoppe (1981), identified the frequency dependence of Pc3 waves on $B_{IMF}$, calculating it as $f(mHz) = (5.81 \pm 0,14)B_{IMF}(nT)$. Le and Russell (1996) further refined this model by incorporating the IMF cone angle, resulting in $f(mHz) = (0.72 + 4.67cos\theta_{Bx})B_{IMF}(nT)$.

Although initially it was presumed that foreshock waves would directly enter the dayside magnetosphere, observational evidence for sinusoidal Pc3 waves in the downstream of quasi-parallel shocks is scarce (e.g., Engebretson et al., 1991). The mechanisms by which these waves propagate from the foreshock into the magnetosphere remain elusive. Recent two-dimensional global hybrid simulations have examined the propagation of Pc3 waves on the equatorial plane (Palmroth et al., 2015; Takahashi et al., 2021; Turc et al., 2018, 2022, 2023). However, the global structure of the foreshock and the coupling of its waves with the magnetospheric system are of three-dimensional (3D) nature, and the Pc3 waves are primarily observed at high latitudes on Earth. Thus, a deeper understanding of the dayside Pc3 wave propagation is required. In this paper, we use a 3D global hybrid simulation at a realistic scale to study the transmission of Pc3 waves through the bow shock, magnetosheath, and magnetosphere under a radial IMF. The structure of this paper is organized as follows. Section 2 describes the simulation model and initial parameters; Section 3 presents the simulation results; and Section 4 offers the conclusions and discussion.

## 2. Simulation Model

This study employs a 3D global hybrid simulation model (Lin & Wang, 2005), where ions are simulated as particles and electrons are modeled as a massless fluid that neutralizes charge. The global hybrid simulation serves as an effective tool for examining interactions between the solar wind and the magnetosphere. In the model, the displacement current is omitted, the electric field is determined using Ohm's law, and the advance of magnetic field is governed by Faraday's law. The simulation is performed in a spherical coordinate system ($r$, θ, φ). The simulation domain consists of $N_r \times N_\theta \times N_\varphi = 720 \times 420 \times 540$ cells in the ranges [$3R_E$, $30R_E$] [$-10^\circ$, $190^\circ$], and [$20^\circ$, $160^\circ$] for ($r$, θ, φ) directions, respectively. The open boundary conditions are used for particles and fields, except a conductive field boundary at the inner boundary ($r = 3R_E$) and an injection of solar wind particles at the outer boundary ($r = 30R_E$). Within the inner magnetosphere ($r \leq 6.5R_E$), a cold, incompressible ion fluid is filled to represent the plasmasphere.

Grid spacing in the radial direction varies, being approximately $0.02R_E$ between $8R_E$ and $14R_E$, and larger outside this range to balance resolution needs against computational costs. The simulation results are presented in geocentric solar-magnetospheric (GSM) coordinates, with the $x$-axis points from the Earth's center to the Sun, the $z$-axis aligned with the Earth's dipole axis, and the $y$-axis completing the right-handed coordinates system. The simulation advances in steps of $\Delta t = 0.02\Omega_i^{-1}$, with $\Omega_i$ representing the ion gyrofrequency determined by the solar wind magnetic field. Initially, the simulation involves about $8 \times 10^9$ macro-particles. The solar wind parameters include the plasma number density of $N_i = 3.2$ cm$^{-3}$, the magnetic field of $\boldsymbol{B} = (3.72, -0.13, 0.21)$nT, and the solar wind velocity of $\boldsymbol{V}_{SW} = (-466.48, -12.86, -14.31)$ km/s. Thus, the inverse of ion gyrofrequency is given as $\Omega_i^{-1} = 2.8$ $s$. The plasma beta for both ions and electrons is $\beta i = \beta e = 0.22$, and the Alfven Mach number

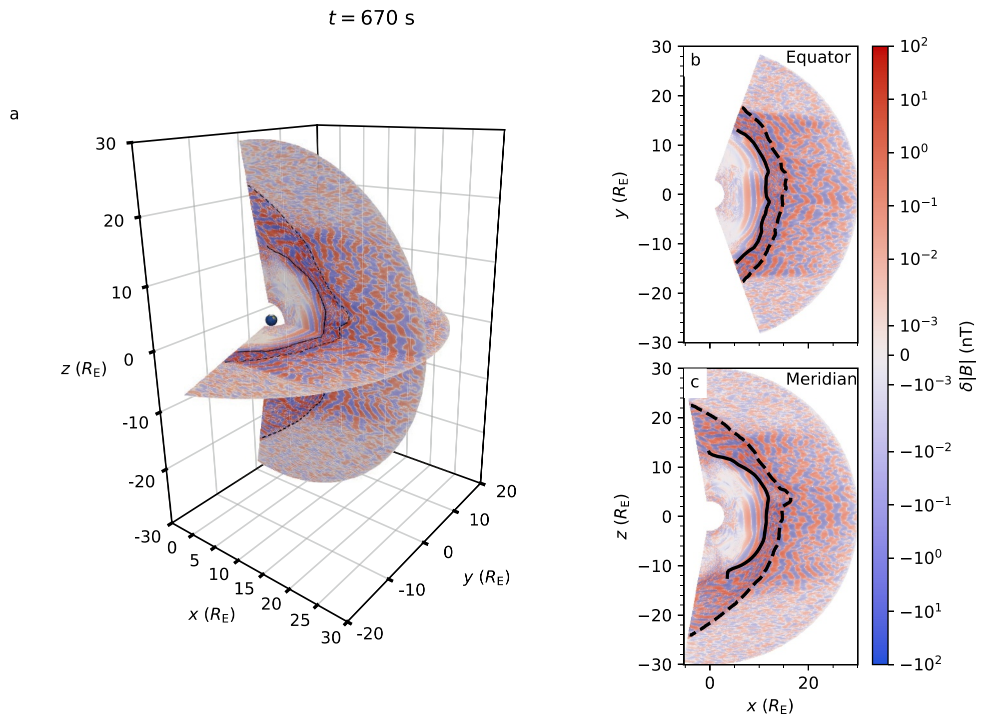


**Figure 1.** Overview of simulation results: the spatial distribution of the fluctuating magnetic fields at $t$ = 670s in the 3D domain (a), the equatorial plane (b), and the meridian plane (c).

is $M_A = 12.27$. The simulation uses a realistic magnetosphere scale where 1 $R_E = 50$ $d_{i0}$, with $d_{i0}$ representing the ion inertial length in the solar wind. These solar wind parameters are maintained constant throughout the simulation. Additionally, there are no incoming fluctuations at the boundaries, and the observed waves are self-consistently generated by shock-reflected particles. The solar wind parameters used in our simulation are based on an event described by Shue et al. (2009), where the IMF was predominantly aligned in the radial direction between 14:15:00 and 14:45:00 UT on 12 August 2007.

## 3. Simulation Results

With the 3D global hybrid simulation model and the initial setup described above, we examine the transmission of dayside Pc3 waves under a radial IMF. An overview of simulation results is shown in Figure 1, which displays the spatial distribution of the fluctuating magnetic fields at $t = 670$s in the 3D domain (Figure 1a), the equatorial plane (Figure 1b), and the meridian plane (Figure 1c). The data for Figure 1 has been bandpass filtered between 10 and 35 mHz. Solid black lines mark the position of magnetopause, while dashed black lines represent the position of bow shock. Intense wave activity is clearly observed from 30 $R_E$ to about 6 $R_E$. As shown in Movies S1 and S2 in the supporting information, fluctuations in the foreshock intensify as they approach the shock, consistent with spacecraft observations (Le & Russell, 1992). Meanwhile, in the magnetosphere, there is a noticeable decline in magnetic field fluctuations as one moves inward, aligning with the expected decrease in compressive wave propagation into the magnetosphere. To emphasize the propagation and evolution of these waves near the shock and magnetopause, Movies S1 and S2 in the supporting information only show the region between 3 RE and 20 RE, rather than the entire simulation domain. Frequency analysis of the disturbed magnetic field indicates a period of approximately 40s, characteristic of the Pc3 frequency band. These Pc3 waves demonstrate substantial variation in wavelength across different regions: the foreshock, magnetosheath, and magnetosphere. Notably, fluctuations in the magnetosheath exhibit significantly shorter wavelengths compared to those in the foreshock and magnetosphere. In the foreshock, the waves extend over several Earth radii in the perpendicular direction. Their propagation direction forms a small angle with the IMF—less than 20°, aligning well with previous satellite observations (Eastwood, Balogh, et al., 2005). Additionally, these waves exhibit a broad distribution in azimuthal and polar angles, covering regions from $-70^\circ$ to $70^\circ$ geomagnetic longitude, and from $-60^\circ$ to $60^\circ$ geomagnetic latitude.

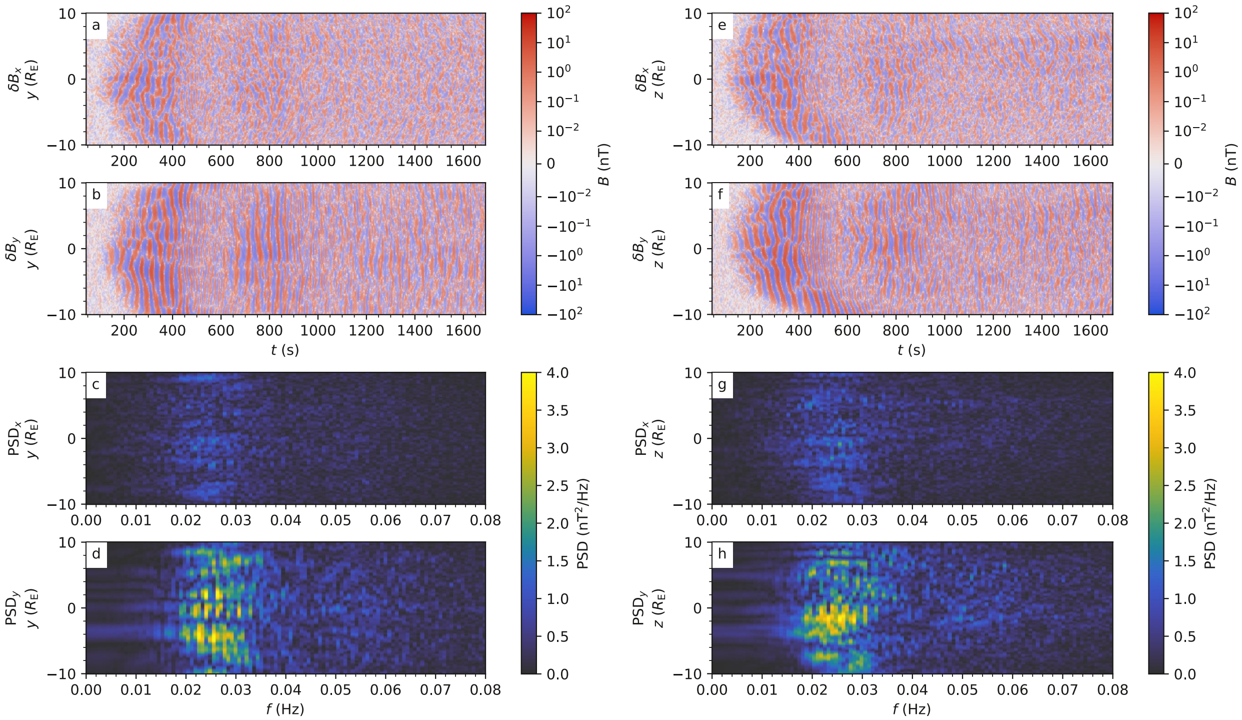


**Figure 2.** Time evolution of fluctuating magnetic fields (a) $\delta B_x$, (b) $\delta B_y$ at (x, z) = ($20R_E$, 0) as a function of $t$ and $y$. PSD of (c) $\delta B_x$, (d) $\delta B_y$ as a function of $f$ and $y$. Time evolution of fluctuating magnetic fields (e) $\delta B_x$, (f) $\delta B_y$ at (x, y) = ($20R_E$, 0) as a function of $t$ and $z$. PSD of (g) $\delta B_x$, (h) $\delta B_y$ as a function of $f$ and $z$.

To verify that the dominate fluctuations in the foreshock are Pc3 waves, we fixed $x$ at $20R_E$ and analyzed the time evolution and power spectral density (PSD) of the magnetic field components $\delta B_x$ and $\delta B_y$ along the $y$ and $z$ axes as illustrated in Figure 2. The frequency distribution of these foreshock waves predominantly ranges between 0.02 and 0.03 Hz (Figures 2d and 2h), closely aligning with the 25 mHz frequency predicted by the observational model under same IMF conditions (Le & Russell, 1996). This confirm the accuracy of our simulation results. For simplicity, the frequency range between 0.02 and 0.03 Hz will be classified as the Pc3 range in this paper, despite a slight extension into the Pc4 range. The analysis revealed that the perpendicular fluctuating magnetic field ($\delta B_y$) was more pronounced than its parallel component ($\delta B_x$), and the waves exhibit right-handed helicity in the plasma frame. This indicates that these waves are quasi-parallel fast magnetosonic waves. In the equatorial plane (Figures 2a and 2b), the wave excitation begins near magnetic noon at $t$ = 100s, with subsequent activations extending to the morning and afternoon sides by $t$ = 200s. A similar pattern is observed in the meridian plane (Figures 2e and 2f), where waves are initially detected at the equator ($t$ = 100s) and later off-equator. There is a clear trend showing that higher latitudes experience later wave activity. Additionally, PSD analysis reveals that wave amplitudes decrease with increasing latitude, providing further insights into the spatial distribution and propagation of these waves.

Figure 3 presents a time-position map of the magnetic fields along the Sun-Earth line. As with Figure 1, the data for this plot has been bandpass filtered within the range of 10–35 mHz. Solid black lines denote the position of the magnetopause, and dashed black lines indicate the bow shock. A comparative analysis of the three magnetic field components reveals that $\delta B_z$ and $\delta B_x$ components can effectively penetrate the magnetosphere, with the $\delta B_z$ component being dominant within the magnetosphere. Within the magnetosheath, the waves display varying slopes, suggesting a decrease in the wave speed after crossing the bow shock. Moreover, it is evident that these waves have smaller spatial scales in the magnetosheath. Since the simulation cover a sufficiently long period, a complete oscillation cycle at the magnetopause are observed, with a period of about 1600s. This closely matches the period of the fundamental frequency of surface waves at the magnetopause (Archer & Plaschke, 2015). Additional analysis of wave activity off the Sun-Earth line shows generally consistent results, though the wave intensity appears slightly weaker.

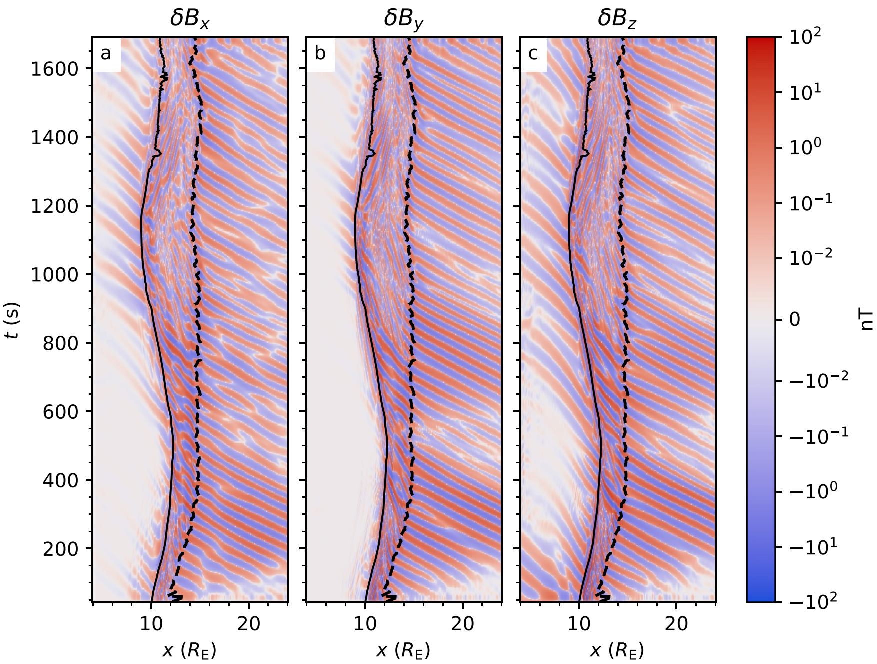


**Figure 3.** Maps of the fluctuating magnetic fields (a) $\delta B_x$, (b) $\delta B_y$, and (c) $\delta B_z$ along the Sun-Earth line as a function of $x$ and $t$.

Figure 4 presents results from virtual spacecraft observations designed to analyze changes in the properties of Pc3 waves as they propagate across different regions: the foreshock (Figures 4a–4d), the magnetosheath (Figures 4e–4h), and the magnetosphere (Figures 4i–4l). The magnetic field components are shown in the mean-field aligned coordinate system, where the perpendicular directions are defined such that $B_{\perp 1}$ lies in the simulation ($x$−$y$) plane

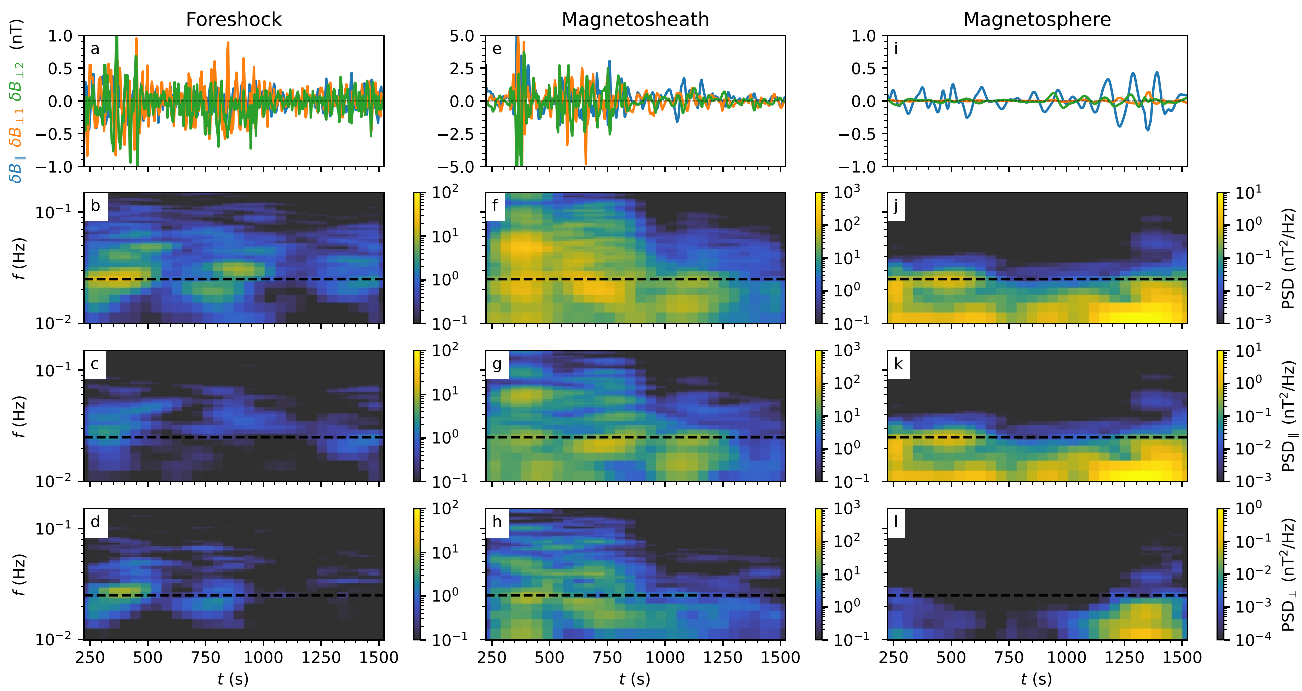


**Figure 4.** (a) Time evolution of fluctuating magnetic fields, and PSD of (b) $\delta|B|$, (c) $\delta B_{\parallel}$, and (d) $B_{\perp}$ in the foreshock ($x = 17R_E$). (e)–(h) and (i)–(l) shows the same format as (a)–(d) except for the magnetosheath ($x = x_{MP} + 0.8R_E$), and the magnetosphere ($x = x_{MP}$ - $0.8R_E$), where $x_{MP}$ is the magnetopause position.

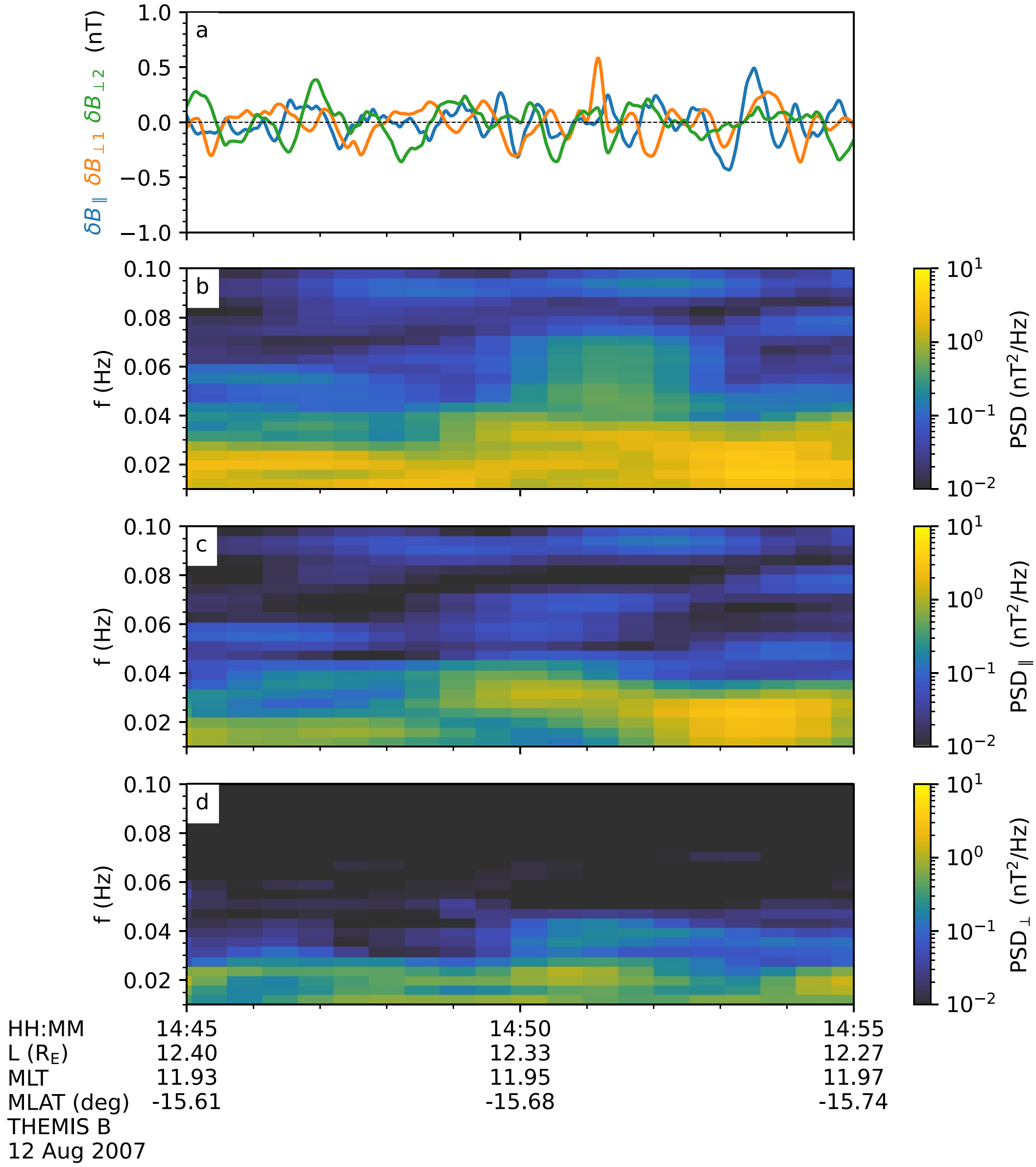


**Figure 5.** THB observations of the Pc3 ULF waves. The magnetic field perturbations in the mean-field aligned coordinate, and power spectral density of the observed magnetic field.

and $B_{\perp 2}$ completes the right-handed set. Black dashed lines in the spectrogram indicates the frequency position at 25 mHz. In the foreshock, the magnetic field perturbations are primarily dominated by the perpendicular component. In the magnetosheath, both perpendicular and parallel components of magnetic field perturbations are substantial, with the parallel components being slightly more pronounced. In the magnetosphere, the fluctuating magnetic field predominantly occur in the parallel direction. Furthermore, only lower frequency fluctuations (below 30 mHz) can be transmitted into the magnetosphere. Compared to the magnetosphere and foreshock, fluctuations in the magnetosheath exhibit a broader spectrum. This broader spectral distribution may account for the scarcity of observational evidence of sinusoidal Pc3 waves in the magnetosheath downstream of quasi-parallel shocks. Figure 5 shows the Pc 3 waves observed by THB satellite in the magnetosphere close to the magnetopause and their wave spectra for the event described by Shue et al. (2009). The dominant wave modes are primarily lower frequency compressional waves (below 30 mHz). This is largely consistent with our simulation results. These observations were made near the magnetopause following an impact by a high-speed jet (Shue et al., 2009), resulting in perpendicular magnetic field disturbances that are slightly stronger than those simulated within the magnetosphere. Overall, our simulations of Pc3 waves within the magnetosphere closely match the satellite observations.

## 4. Conclusions and Discussion

In this paper, we employed a 3D global hybrid simulation at a realistic scale to investigate the transmission of dayside ULF waves under a radial IMF. The Alfven Mach number $M_A$ in our simulation is 12.27. The Pc3 waves are self-consistently generated in the foreshock region and transmitted into the magnetosheath and magnetosphere. These waves exhibit a broad distribution in azimuthal and polar angles, covering regions from $-70^{\circ}$ to $70^{\circ}$ geomagnetic longitude, and from $-60^{\circ}$ to $60^{\circ}$ geomagnetic latitude. In the foreshock, the fluctuations predominantly occur perpendicular to the background magnetic field and exhibit right-handed helicity in the plasma frame, indicating that they are quasi-parallel fast magnetosonic waves. In the magnetosphere, the fluctuations are primarily along the parallel direction, suggesting that the dominant wave mode are compressional. Notably, the wave spectrum in the magnetosheath is broader compared to those in the magnetosphere and foreshock. This broader spectrum may explain the limited observational evidence of sinusoidal Pc3 waves in the magnetosheath downstream of quasi-parallel shocks. Additionally, our findings suggest that only waves with frequencies below 30 mHz are effectively transmitted into the magnetosphere.

Numerical studies of Pc3 waves are challenging as these waves originate from ion kinetic instability and require 3D model to simulate their interaction with field line resonances (FLRs) (Chen & Hasegawa, 1974; Southwood, 1974). Most global simulations of ULF waves utilized the magnetohydrodynamic (MHD) framework (Archer et al., 2022; Claudepierre et al., 2010; Ellington et al., 2016), which results in these fluctuations not being self-consistently excited in the simulations. On the other hand, studies based on local hybrid models cannot provide the global propagation and evolution characteristics of Pc3 waves in the foreshock and magnetosphere (Hao et al., 2021; Krauss-Varban, 1995; Krauss-Varban & Omidi, 1991). Recent studies based on 2D global hybrid simulation have investigated the transmission of Pc3 waves on the equator (Palmroth et al., 2015; Takahashi et al., 2021; Turc et al., 2018, 2022, 2023). The equatorial 2D configuration complicates the identification of the magnetopause position and results in an increased IMF pileup ahead of the dayside magnetosphere. This effect drives a continuous outward motion of the bow shock and pushes the magnetopause closer to Earth. Consequently, the thickness of the magnetosheath could be overestimated in 2D simulations, which may artificially hinder the transmission of waves from the foreshock to the magnetosphere. In our 3D simulation, which is scaled realistically, the thickness of the magnetosheath is reliable. Therefore, the propagation of Pc3 fluctuations across the shock and through magnetosheath is not artificially hindered. Additionally, 3D simulations offer a more advantageous perspective for examining the evolution of Pc3 fluctuations in high-latitude regions, an analysis not possible with 2D simulations.

The spatial resolution in our simulation is comparable to the proton inertial length in the solar wind, which should not impact the phenomena of interest here since the wavelength of Pc3 waves ($\sim R_E$) is much larger than the grid resolution ($0.02R_E$). In the magnetosheath, we observed significant wave power at small scales and higher frequencies. This phenomenon arises because our simulation captures not only waves originating from the foreshock and the quasi-parallel shock but also various wave modes generated locally in the magnetosheath. In our study, we focus on the transmission of Pc3 fluctuations within the foreshock, magnetosheath, and magnetosphere. Disturbances originating from the foreshock are theoretically known to propagate into the magnetosphere, driving toroidal Alfvén waves (FLRs) through a direct mode conversion process. Although previous 3D global hybrid simulations conducted at a reduced scale, such as those by Lin and Wang (2005) and Shi et al. (2021), have successfully modeled FLRs, our simulations did not observe these waves. This absence is due to our specific density settings in the magnetosphere, which do not match the frequencies of Pc3 fluctuations and consequently place the occurrence of FLRs outside our simulated area. Moreover, Ofman et al. (2021) has revealed that alpha particles in the solar wind play a significant role in magnetic and density structures of high Mach number shocks. Based on these insights, our future work will include adjustments to the density settings within a realistic magnetosphere to better capture the generation and propagation of FLRs and further explore the impact of alpha particles on Pc3 wave dynamics in the foreshock and magnetosheath.

## Data Availability Statement

The simulation data (Ren, 2024) used to plot the figures in this paper can be downloaded from "National Space Science Data Center, National Science and Technology Infrastructure of China", https://www.scidb.cn/en/detail?dataSetId=e920437796a54f8f87c244e38d59501e, doi:10.57760/sciencedb.09249.

**Acknowledgments**
This work was supported by the National Natural Science Foundation of China (42130210, 42204169), and the National Key Research and Development Program of China (2023YFC2808905).

## References

Archer, M., Horbury, T. S., Lucek, E. A., Mazelle, C., Balogh, A., & Dandouras, I. (2005). Size and shape of ULF waves in the terrestrial foreshock. *Journal of Geophysical Research*, *110*(A5), A05208. https://doi.org/10.1029/2004JA010791

Archer, M. O., & Plaschke, F. (2015). What frequencies of standing surface waves can the subsolar magnetopause support? *Journal of Geophysical Research: Space Physics*, *120*(5), 3632–3646. https://doi.org/10.1002/2014JA020545

Archer, M. O., Southwood, D. J., Hartinger, M. D., Rastaetter, L., & Wright, A. N. (2022). How a realistic magnetosphere alters the polarizations of surface, fast magnetosonic, and Alfvén waves. *Journal of Geophysical Research: Space Physics*, *127*(2), e2021JA030032. https://doi.org/10.1029/2021JA030032

Bier, E. A., Owusu, N., Engebretson, M. J., Posch, J. L., Lessard, M. R., & Pilipenko, V. A. (2014). Investigating the IMF cone angle control of Pc3-4 pulsations observed on the ground. *Journal of Geophysical Research: Space Physics*, *119*(3), 1797–1813. https://doi.org/10.1002/2013JA019637

Burgess, D. (1995). Foreshock–shock interaction at collisionless quasi-parallel shocks. *Advances in Space Research*, *15*(8–9), 159–169. https://doi.org/10.1016/0273-1177(94)00098-l

Chen, L., & Hasegawa, A. (1974). A theory of long-period magnetic pulsations: 1. Steady state excitation of field line resonance. *Journal of Geophysical Research*, *79*(7), 1024–1032. https://doi.org/10.1029/JA079i007p01024

Chi, P. J., Russell, C. T., & Le, G. (1994). Pc 3 and Pc 4 activity during a long period of low interplanetary magnetic field cone angle as detected across the Institute of Geological Sciences Array. *Journal of Geophysical Research*, *99*(A6), 11127–11139. https://doi.org/10.1029/94JA00517

Claudepierre, S. G., Hudson, M. K., Lotko, W., Lyon, J. G., & Denton, R. E. (2010). Solar wind driving of magnetospheric ULF waves: Field line resonances driven by dynamic pressure fluctuations. *Journal of Geophysical Research*, *115*(A11), A11202. https://doi.org/10.1029/2010JA015399

Eastwood, J. P., Balogh, A., Lucek, E. A., Mazelle, C., & Dandouras, I. (2005). Quasi-monochromatic ULF foreshock waves as observed by the four-spacecraft cluster mission: 2. Oblique propagation. *Journal of Geophysical Research*, *110*(A11), A11220. https://doi.org/10.1029/2004JA010618

Eastwood, J. P., Lucek, E. A., Mazelle, C., Meziane, K., Narita, Y., Pickett, J., & Treumann, R. A. (2005). The foreshock. *Space Science Reviews*, *118*(1–4), 41–94. https://doi.org/10.1007/s11214-005-3824-3

Ellington, S. M., Moldwin, M. B., & Liemohn, M. W. (2016). Local time asymmetries and toroidal field line resonances: Global magnetospheric modeling in SWMF. *JGR. Space Physics*, *121*(3), 2033–2045. https://doi.org/10.1002/2015JA021920

Engebretson, M. J., Lin, N., Baumjohann, W., Luehr, H., Anderson, B. J., Zanetti, L. J., et al. (1991). A comparison of ULF fluctuations in the solar wind, magnetosheath, and dayside magnetosphere, 1, Magnetosheath morphology. *Journal of Geophysical Research*, *96*(A3), 3441–3454. https://doi.org/10.1029/90JA02101

Engebretson, M. J., Zanetti, L. J., Potemra, T. A., Baumjohann, W., Lühr, H., & Acuna, M. H. (1987). Simultaneous observation of Pc 3-4 pulsations in the solar wind and in the Earth's magnetosphere. *Journal of Geophysical Research*, *92*(10), 10053–10062. 053–10,062. https://doi.org/10.1029/JA092iA09p10053

Greenstadt, E. W., & Mellott, M. M. (1985). Variable field-to-normal shock-foreshock boundary observed by ISEE-1 and -2. *Geophysical Research Letters*, *12*(3), 129–132. https://doi.org/10.1029/gl012i003p00129

Hao, Y. Q., Lu, D., Wu, S., Lu, L., Xiang, L., & Ke, Y. (2021). Low-frequency waves upstream of quasi-parallel shocks: Two-dimensional hybrid simulations. *The Astrophysical Journal*, *915*(1), 64. https://doi.org/10.3847/1538-4357/ac02ce

Heilig, B., Lühr, H., & Rother, M. (2007). Comprehensive study of ULF upstreamwaves observed in the topside ionosphere by CHAMP and on the ground. *Annals of Geophysics*, *25*(3), 737–754. https://doi.org/10.5194/angeo-25-737-2007

Hoppe, M. M., & Russell, C. T. (1983). Plasma rest frame frequencies and polarizations of low-frequency upstream waves: ISEE 1 and 2 observations. *Journal of Geophysical Research*, *88*, 2021–2028.

Krauss-Varban, D. (1995). Waves associated with quasi-parallel shocks: Generation, mode conversion and implications. *Advances in Space Research. Proceedings of the D2.1 symposium of COSPAR scientific commission D*, *15*(8), 271–284. https://doi.org/10.1016/0273-1177(94)00107-c

Krauss-Varban, D., & Omidi, N. (1991). Structure of medium Mach number quasi-parallel shocks: Upstream and downstream waves. *Journal of Geophysical Research*, *96*(A10), 17715–17731. https://doi.org/10.1029/91JA01545

Le, G., & Russell, C. (1992). A study of ULF wave foreshock morphology—II: Spatial variation of ULF waves. *Planetary and Space Science*, *40*(9), 1215–1225. https://doi.org/10.1016/0032-0633(92)90078-3

Le, G., & Russell, C. (1996). Solar wind control of upstream wave frequency. *Journal of Geophysical Research*, *101*(A2), 2571–2575. https://doi.org/10.1029/95JA0315

Lin, Y., & Wang, X. (2005). Three-dimensional global hybrid simulation of dayside dynamics associated with the quasi-parallel bow shock. *Journal of Geophysical Research*, *110*(A12), A12216. https://doi.org/10.1029/2005JA011243

Liu, T. Z., Hao, Y., Wilson, L. B., Turner, D. L., & Zhang, H. (2021). Magnetospheric Multiscale observations of Earth's oblique bow shock reformation by foreshock ultra-low-frequency waves. *Geophysical Research Letters*, *48*(2), e91184. https://doi.org/10.1029/2020gl091184

Motoba, T., Ebihara, Y., Ogawa, Y., Kadokura, A., Engebretson, M. J., Angelopoulos, V., et al. (2019). On the driver of daytime Pc3 auroral pulsations. *Geophysical Research Letters*, *46*(2), 553–561. https://doi.org/10.1029/2018GL080842

Ofman, L., Wilson III, L. B., Koval, A., & Szabo, A. (2021). Oblique high Mach number heliospheric shocks: The role of αparticles. *Journal of Geophysical Research: Space Physics*, *126*(5), e2020JA028962. https://doi.org/10.1029/2020JA028962

Palmroth, M., Archer, M., Vainio, R., Hietala, H., Pfau-Kempf, Y., Hoilijoki, S., et al. (2015). ULF foreshock under radial IMF: THEMIS observations and global kinetic simulation vlasiator results compared. *Journal of Geophysical Research: Space Physics*, *120*(10), 8782–8798. https://doi.org/10.1002/2015JA021526

Regi, M., De Lauretis, M., & Francia, P. (2014). The occurrence of upstream waves in relation with the solar wind parameters: A statistical approach to estimate the size of the foreshock region. *Planetary and Space Science*, *90*, 100–105. https://doi.org/10.1016/j.pss.2013.10.012

Ren, J. (2024). Data for "the transmission of Pc 3 waves from the foreshock into the Earth's magnetosphere: 3D global hybrid simulation" [Dataset]. *Science Data Bank*. Retrieved from https://doi.org/10.57760/sciencedb.09249

Russell, C. T., & Hoppe, M. M. (1981). The dependence of upstream wave periods on the interplanetary magnetic field strength. *Geophysical Research Letters*, *8*(6), 615–617. https://doi.org/10.1029/GL008i006p00615

Shi, F., Lin, Y., Wang, X., Wang, B., & Nishimura, Y. (2021). 3-D global hybrid simulations of magnetospheric response to foreshock processes. *Earth Planets and Space*, *73*(1), 138. https://doi.org/10.1186/s40623-021-01469-2

Shue, J.-H., Chao, J.-K., Song, P., McFadden, J. P., Suvorova, A., Angelopoulos, V., et al. (2009). Anomalous magnetosheath flows and distorted subsolar magnetopause for radial interplanetary magnetic fields. *Geophysical Research Letters*, *36*(18), L18112. https://doi.org/10.1029/2009GL039842

Southwood, D. J. (1974). Some features of field line resonances in the magnetosphere, Planet. *Space Science*, *22*(3), 483–491. https://doi.org/10.1016/0032-0633(74)90078-6

Takahashi, K., McPherron, R. L., & Terasawa, T. (1984). Dependence of the spectrum of Pc 3–4 pulsations on the interplanetary magnetic field. *Journal of Geophysical Research*, *89*(A5), 2770–2780. https://doi.org/10.1029/JA089iA05p02770

Takahashi, K., Turc, L., Kilpua, E., Takahashi, N., Dimmock, A., Kajdic, P., et al. (2021). Propagation of ultra-low-frequency waves from the ion foreshock into the magnetosphere during the passage of a magnetic cloud. *Journal of Geophysical Research: Space Physics*, *126*(2), e2020JA028474. https://doi.org/10.1029/2020JA028474

Turc, L., Ganse, U., Pfau-Kempf, Y., Hoilijoki, S., Battarbee, M., Juusola, L., et al. (2018). Foreshock properties at typical and enhanced interplanetary magnetic field strengths: Results from hybrid-vlasov simulations. *Journal of Geophysical Research: Space Physics*, *123*(7), 5476–5493. https://doi.org/10.1029/2018JA025466

Turc, L., Roberts, O. W., Verscharen, D., Dimmock, A. P., Kajdič, P., Palmroth, M., et al. (2023). Transmission of foreshock waves through Earth's bow shock. *Nature Physics*, *19*(1), 78–86. https://doi.org/10.1038/s41567-022-01837-z

Turc, L., Zhou, H., Tarvus, V., Ala-Lahti, M., Battarbee, M., Pfau-Kempf, Y., et al. (2022). A global view of Pc3 wave activity in near-Earth space: Results from hybrid-Vlasov simulations. *Frontiers Astronomy Space Science*, *9*, 989369. https://doi.org/10.3389/fspas.2022.989369

Wilson, L. B., III. (2016). Low frequency waves at and upstream of collisionless shocks. *Washington DC American: Geophysical Union Geophysical Monograph Series*, *216*, 269–291. https://doi.org/10.1002/9781119055006.ch16

Wu, M., Hao, Y., Lu, Q., Huang, C., Guo, F., & Wang, S. (2015). The role of large amplitude upstream low-frequency waves in the generation of superthermal ions at a quasi-parallel collisionless shock: Cluster observations. *The Astrophysical Journal*, *808*(1), 2. https://doi.org/10.1088/0004-637x/808/1/2

Yeoman, T. K., Wright, D. M., Engebretson, M. J., Lessard, M. R., Pilipenko, V. A., & Kim, H. (2012). Upstream-generated Pc3 ULF wave signatures observed near the Earth's cusp. *Journal of Geophysical Research*, *117*(A3), A03202. https://doi.org/10.1029/2011JA017327

Yumoto, K., Saito, T., Akasofu, S.-I., Tsurutani, B. T., & Smith, E. J. (1985). Propagation mechanism of daytime Pc 3–4 pulsations observed at synchronous orbit and multiple ground-based stations. *Journal of Geophysical Research*, *90*(A7), 6439–6450. https://doi.org/10.1029/JA090iA07p06439

Yumoto, K., Saito, T., Tsurutani, B. T., Smith, E. J., & Akasofu, S.-I. (1984). Relationship between the IMF magnitude and Pc3 magnetic pulsations in the magnetosphere. *Journal of Geophysical Research*, *89*(A11), 9731–9740. https://doi.org/10.1029/JA089iA11p09731